

Rate dependence of dry, oil- or water-saturated chalk

Andreassen, Katrine Alling; Al-Alwan, A.

Publication date:
2015

Document Version
Publisher's PDF, also known as Version of record

[Link back to DTU Orbit](#)

Citation (APA):

Andreassen, K. A., & Al-Alwan, A. (2015). Rate dependence of dry, oil- or water-saturated chalk. Paper presented at 49th US Rock Mechanics / Geomechanics Symposium, San Francisco, United States.

DTU Library

Technical Information Center of Denmark

General rights

Copyright and moral rights for the publications made accessible in the public portal are retained by the authors and/or other copyright owners and it is a condition of accessing publications that users recognise and abide by the legal requirements associated with these rights.

- Users may download and print one copy of any publication from the public portal for the purpose of private study or research.
- You may not further distribute the material or use it for any profit-making activity or commercial gain
- You may freely distribute the URL identifying the publication in the public portal

If you believe that this document breaches copyright please contact us providing details, and we will remove access to the work immediately and investigate your claim.

Rate dependence of dry, oil- or water-saturated chalk

Andreassen, K.A.

Technical University of Denmark, Kgs. Lyngby, Denmark

Al-Alwan, A.

Formerly Technical University of Denmark, Kgs. Lyngby, Denmark

Copyright 2015 ARMA, American Rock Mechanics Association

This paper was prepared for presentation at the 49th US Rock Mechanics / Geomechanics Symposium held in San Francisco, CA, USA, 28 June-1 July 2015.

This paper was selected for presentation at the symposium by an ARMA Technical Program Committee based on a technical and critical review of the paper by a minimum of two technical reviewers. The material, as presented, does not necessarily reflect any position of ARMA, its officers, or members. Electronic reproduction, distribution, or storage of any part of this paper for commercial purposes without the written consent of ARMA is prohibited. Permission to reproduce in print is restricted to an abstract of not more than 200 words; illustrations may not be copied. The abstract must contain conspicuous acknowledgement of where and by whom the paper was presented.

ABSTRACT: The rate dependence of dry, oil- or water-saturated high-porosity outcrop chalk is investigated based on whether the fluid effect could be excluded from a governing material parameter, the b-factor. The b-factor is used in geotechnical engineering to establish the difference in evolution of load between stress-strain curves when applying different loading rates. The material investigated is outcrop chalk from Stevns, Southern part of Denmark, with a porosity of 43 to 44% and subjected to varying loading rates. The Biot critical frequency is a function of the fluid properties viscosity and density, and the material properties porosity and permeability. The critical frequency is interpreted as a measure of the solid-fluid friction and hence relevant to use for subtracting the fluid effect to arrive at a pure material parameter. The results show a correlation between the b-factor and the Biot critical frequency.

1. INTRODUCTION

For hydrocarbon reservoir behavior upscaling from laboratory results to field behavior is important. One of the central parameters which are challenging to apply in the laboratory is the low strain or stress rate involved. These can range from as much as 1 %/hour for the laboratory tests to 10^{-4} %/hour for a hydrocarbon reservoir under depletion [1]. Thus an upscaling encompasses an order of magnitude four for any effect from this parameter. The time dependence is important as it affects both the strength and the deformation such that a slow loading results in a weaker material response and a faster loading rate yields a higher strength and a stiffer response.

Dealing with the time effect is exemplified by Rhett [2] for the Ekofisk Field, and by de Waal and Smits [3] for Goose Creek, Wilmington, Inglewood, Nigata, Boliva coast, and Groningen fields.

The physical reasoning behind observed rate dependence varies from specific material changes to rheological effects and to chemical influences. Many turn to an explanation of material changes, e.g. Johnson and Rhett [4], who couple deformation with mechanical translation and rotation of fragments. Addis and Jones [5] argue higher stress leads to destructuring of the chalk with

bond breakage, grain crushing, and inter-particle slip. Also Andersen et al. [6] argue that friction between asperities (contact points) explains the rate dependence. Recently, Bhandari and Inoue [7] state that the mechanism for the difference in strain rates is related to stress distribution and damage/failure of specimen due to breaking of cementation and particle crushing and rearranging.

Rheological effects by simplifying the material behavior to a dashpot unit belongs in the framework of viscoplasticity. It is covered among others by De Gennaro et al. [8] where they consider a faster loading rate implies excess pore pressure. This is also applied by Dahou et al. [9] investigating transient creep of porous chalk. The creep behavior of weak rock studied by Maranini [10] also falls within viscoplastic modelling, where the failure and plasticization is dependent on the loading history.

Chemical effects, such as intergranular pressure solution, are believed to affect the deformation and rate dependence as seen by Zhang and Spiers [11], who additionally state that the observed deformation depends on grain size and hence specific surface.

When dealing with time effects, the ultimate limit is constant load, which marks the lower boundary for the

rate dependence with $\frac{d\sigma}{dt} = 0$ corresponding to a creep phase. In such a phase the material is allowed to deform and in effect similar to a very slow loading rate. Consequently the material responds as a weaker material and creeps. This deformation could ultimately result in failure and this leads to dividing into transient–steady state–accelerating creep regimes is first mentioned by Andrade [12] for metal wires under constant tensional load. These regimes are commonly used in compression tests in rock mechanics with steady state and accelerating creep regimes present at higher confining stresses [13, 14]. Boresi and Schmidt [15] comment on the later use of these regimes as valid for constant tensile stress. Pharr and Ashby [16] observe tertiary creep on porous KCl in water or methanol solutions. They suggest that the temperature influenced creep rate is correlated with the fluid viscosity and KCl solubility. Johnson and Rhett [4] and later Andersen et al. [6] observe no tertiary creep (accelerated creep leading to failure) – only transient creep.

To sum up the effects – from either application of varying strain/loading rates or performing creep phases – give rise to observing a time dependent behavior. Physical explanations as listed above could attribute to this phenomenon.

The scope of this paper is to quantitatively describe the material related time dependence for a single type of material. It focuses on separating the effect of different fluids from the time dependence to uniquely define the material dependence. As such the aim is to perform tests on plugs from the same block of material and with the same test program but either water-saturated, oil-saturated or dry.

We hypothesize that the time dependence could be characterized by a pure material-dependent parameter, where the fluid influence is quantified by basic fluid parameters, such as density and viscosity.

2. MATERIAL AND METHOD

The material investigated is outcrop chalk from Stevns, Southern part of Denmark. This type of chalk serves as an analogue in rock mechanical tests for the North Sea high-porosity reservoir chalk. The carbonate content is high, reaching 99%. The chalk is essentially made of skeletal carbonate, originally from the unicellular coccolithophorid algae, which is constructed of small platelets formed into assemblages of rings and rosettes called coccoliths. The basic building block of chalk is therefore the platelet, Sulak and Danielsen [17], and the chalk is formed as a micro-debris of platelets, which can be more or less cemented.

The chalk used in this investigation was sampled as blocks from the Stevns chalk quarry and then cut to

plugs with diameter of 1 inch and height of 2 inches. Then the plugs were characterized with measurements of porosity, permeability and specific surface. The two first found by Poroperm equipment with application of Boyle-Mariotte's principle and gas flow with the Klinkenberg method. The latter found from the BET method by using an Autosorb iQ-AG. Table 1 summarizes the results in section 4.

A number of the plugs were then either left dry, saturated with equilibrated water or saturated with isopar-L laboratory oil. Next, they were subjected to alternating loading rates from 0.003 kN/min to 0.060 kN/min and short creep phases. The test type was unconfined compression. The deformation was recorded by digital image correlation equipment and hence it had to be unconfined. Additionally, the strain and stress output is recorded through the controller of the electro-mechanical load frame. For the water-saturated specimens the base was placed in water in a clear container covered by plastic wrapping on the top. This was done to minimize the evaporation from the specimen as much as possible during the length of the experiment.

The viscoplastic or hypoplastic nature of soft porous rock, such as this high-porosity chalk, calls for using the time dependent concepts from soil mechanics, which follow in the next section.

3. THEORY

For rate dependent behavior, Mesri and Godlewski [18] apply first the secondary strain (measured during a creep phase, where the load is held constant while the strain is recorded)

$$\varepsilon_s = \frac{d\varepsilon}{d(\log(t))}, \quad (1)$$

and then they apply the compression index (measured from the stress-strain curve)

$$Q = \frac{d\varepsilon}{d(\log(\sigma))}, \quad (2)$$

to arrive at the b-factor:

$$b = \frac{\varepsilon_s}{Q} = \frac{d(\log(\sigma))}{d(\log(t))}. \quad (3)$$

where ε is strain, t is time, σ is stress, and b is a material constant, the b-factor. Thus it combines the strain evolution with respect to time and with respect to stress.

Similarly to this, de Waal [19] applied the factor to sandstone where the underlying theory originates from Kolybas [20] as:

$$\dot{\sigma}_z = \frac{\dot{\varepsilon}_z}{c_m} + b \sigma_z \frac{\dot{\varepsilon}_z}{\varepsilon_z}, \quad (4)$$

with $\dot{\epsilon}$ the strain rate, $\dot{\sigma}$ the stress rate, $\ddot{\epsilon}$ the strain acceleration, and c_m the uniaxial compressibility. This is strictly covering compaction. It will here be assumed that for each material the Poisson ratio can be assumed constant throughout a test and that the procedure to measure the b-factor is unaffected by lateral expansion. Indeed the formulation by de Waal [18] leads to

$$c_m(\dot{\sigma}_{z,2}) = c_m(\dot{\sigma}_{z,1}) \left(\frac{\dot{\sigma}_{z,2}}{\dot{\sigma}_{z,1}} \right)^b \quad (5)$$

for two different loading rates, $\dot{\sigma}_{z,1}$ and $\dot{\sigma}_{z,2}$, which show that the relation could also relate to an unconfined tests if the Poisson ratio is independent of loading rate.

For the recent theory and details on hypoplastic behavior consult [21].

For infinitesimal stress changes Eq. 4 gives [18]

$$d\sigma_z = \frac{d\epsilon_z}{c_m} + b \sigma_z d(\ln \dot{\epsilon}_z), \quad (6)$$

and through algebraic manipulation and by assuming non-linearity for the virgin compaction curve de Waal [18] arrives at

$$b = \frac{\ln\left(\frac{\sigma_{z,2}}{\sigma_{z,1}}\right)}{\ln\left(\frac{\dot{\sigma}_{z,2}}{\dot{\sigma}_{z,1}}\right)}. \quad (7)$$

Graphically, applying alternating loading rates result in Figure 1 and Eq. 7 includes these parameters. Consequently, a larger b-factor signifies a material that weakens more from applying identical load rates than compared with a material with lower b-factor.

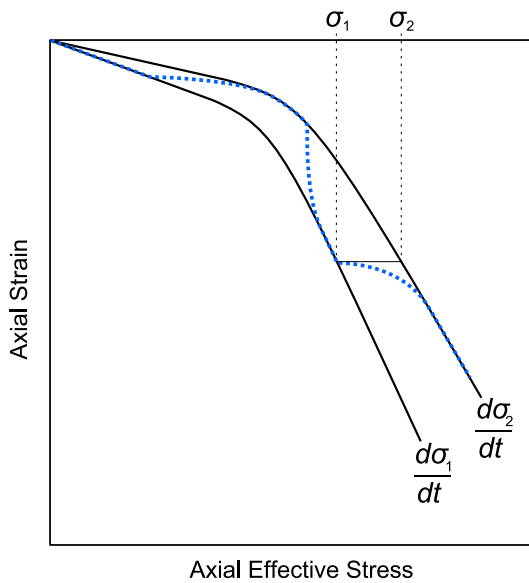


Fig. 1. Graphical overview of the parameters needed to calculate the b-factor.

Now, the b-factor is used in soil mechanics to cover the material behavior and a natural extension would be to

introduce the effect of changing the pore fluid in the pore space to another type with other physical parameters, e.g. density and viscosity.

Bourbié et al. [22, p. 79] discusses the dissipative nature build into the Biot theory and generalize that the Biot critical frequency is a measure of the friction on the small scale – in other words: it is a solid-fluid friction. The definition of the Biot critical frequency, f_c , (often also termed characteristic, cross-over, or reference frequency) is

$$f_c = \frac{\varphi \eta}{2\pi \rho_f k}, \quad (8)$$

where φ is porosity, η is the fluid absolute viscosity, ρ_f is fluid density, and k is absolute permeability. The Biot critical frequency is the limit between a low frequency regime with the pore fluid subjected to viscous forces and a high frequency regime with inertial forces dominating the fluid motion [23, 24], Figure 2. These regimes have been proven experimentally by Johnson et al. [25]. The drag that the solid motion makes on the fluid and whether this is in the viscous or inertial regime is a matter of friction between the liquid and the solid. Bourbié et al. [22, p. 80] list the critical frequency for various materials and pore fluids. Fabricius et al. [26] find the amount of softening of elastic modulus to be correlated with the Biot critical frequency.

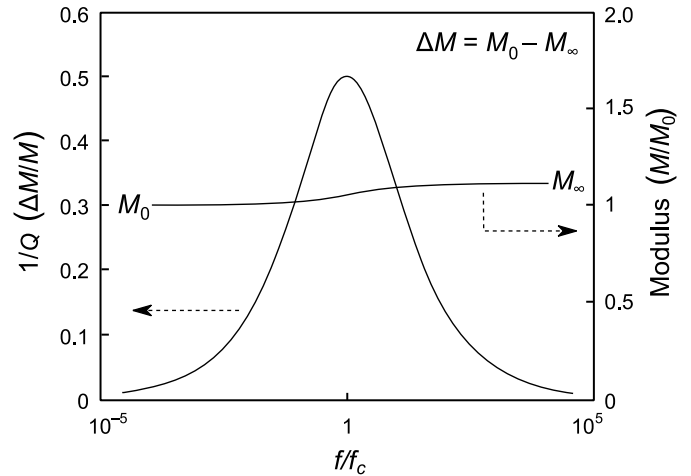


Fig. 2. Representation of Biot critical frequency, modified from [27]. Normalized frequency vs. attenuation or p-wave modulus.

The yield point results from a large set of laboratory results for high-porosity outcrop chalk indicate the following empirical relation [28]:

$$\ln(\sigma_{z, \text{yield}}) = 0.79 \tilde{f}_c^{-0.466} \ln\left(t_{\text{ref}} \frac{d\sigma_z}{dt}\right) + \ln(26.05 \text{ MPa}), \quad (9)$$

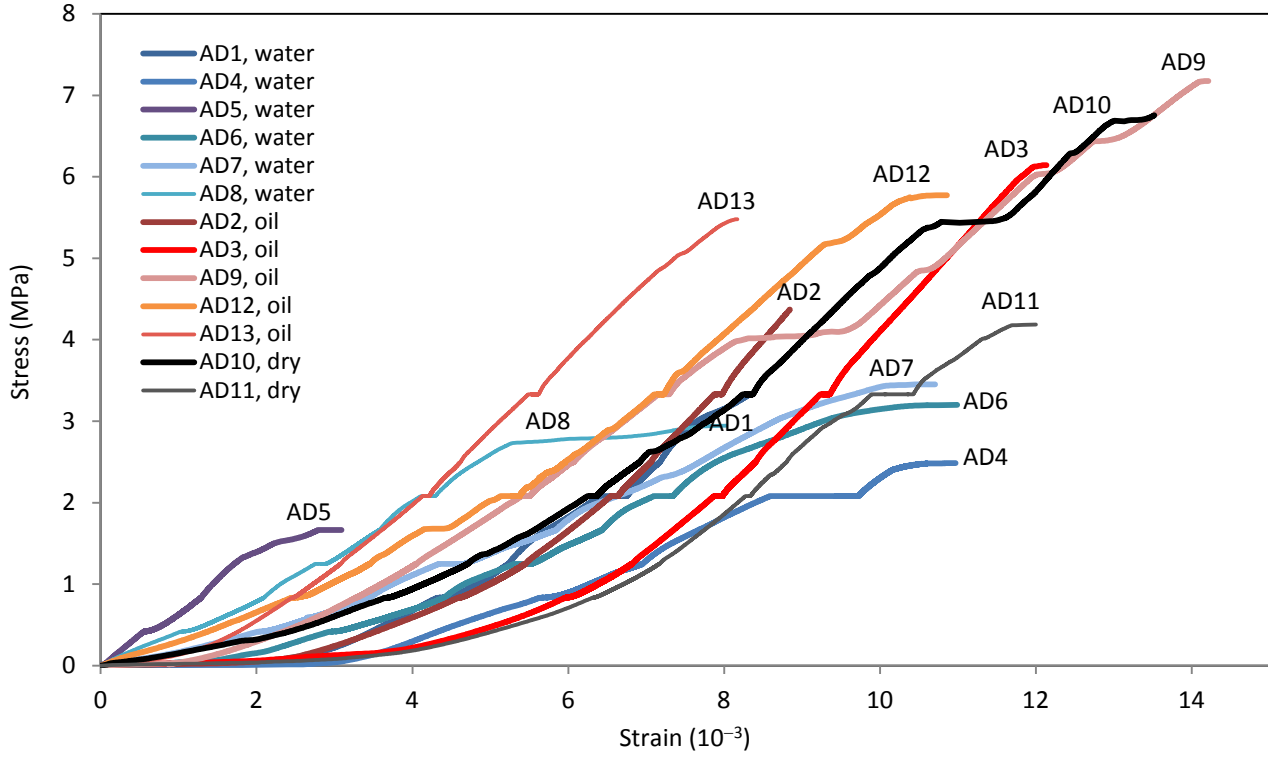


Fig. 3. All stress-strain curves for the performed experiments.

where t_{ref} is a reference time of 1 s introduced to make the units consistent. The normalized critical frequency, \tilde{f}_c , is found from dividing the critical frequency with $f_{ref} = 583260 \text{ s}^{-1}$ [28]. This value is based on the density and viscosity of water at 20°C and a viscous skin depth of 0.74 μm , which is the average pore diameter for Liège chalk [29].

Manipulation of Eq. 9 gives

$$\ln\left(\frac{\sigma_{z, \text{yield}}}{26.05 \text{ MPa}}\right) = 0.79 \tilde{f}_c^{-0.466} \ln\left(t_{ref} \frac{d\sigma_z}{dt}\right). \quad (10)$$

Then taking this equation for two distinct loading rates and subtracting them gives

$$\ln\left(\frac{\frac{\sigma_{z, \text{yield},2}}{26.05 \text{ MPa}}}{\frac{\sigma_{z, \text{yield},1}}{26.05 \text{ MPa}}}\right) = \ln\left(\frac{(t_{ref} \dot{\sigma}_{z,2})^{0.79} \tilde{f}_c^{-0.466}}{(t_{ref} \dot{\sigma}_{z,1})^{0.79} \tilde{f}_c^{-0.466}}\right), \quad (11)$$

with

$$\ln\left(\frac{\sigma_{z, \text{yield},2}}{\sigma_{z, \text{yield},1}}\right) = 0.79 \tilde{f}_c^{-0.466} \ln\left(\frac{\dot{\sigma}_{z,2}}{\dot{\sigma}_{z,1}}\right). \quad (12)$$

Finally, the b-factor could be calculated as

$$b = 0.79 \tilde{f}_c^{-0.466}. \quad (13)$$

4. RESULTS

The results from interchanging the load rates give the curves in Figure 3 for all tests. Table 1 lists the specimen details and b-factor results from measurements of the difference in the stress level between the stress-strain curves and the value of the applied load rates.

Table 1. Specimen details of porosity, permeability, specific surface area, and b-factor.

No.	Fluid	ϕ	k (10^{-15} m^2)	SSA (m^2/g)	b- factor
AD1	Water	0.44	3.44	1.61	0.045
AD2	Oil	0.44	3.11	1.70	0.014
AD3	Oil	0.45	3.16	1.78	0.013
AD4	Water	0.43	2.46	1.81	0.041
AD5	Water	0.45	4.83	1.44	0.049
AD6	Water	0.45	4.82	1.44	0.026
AD7	Water	0.44	3.14	1.69	0.034
AD8	Water	0.44	2.99	1.73	0.033
AD9	Oil	0.44	3.43	1.62	0.019
AD10	Dry	0.44	2.88	1.76	0.010
AD11	Dry	0.44	2.87	1.77	0.009
AD12	Oil	0.44	3.82	1.53	0.016
AD13	Oil	0.44	2.66	1.84	0.017

Figure 4 gives the main result is from the b-factor measurements and calculations. Dashed lines mark an area where all results are included. Higher b-factors correlate with lower normalized Biot critical frequencies.

Results from previous tests on Liege chalk show another correlation and this must be interpreted as the material has another underlying material dependence for the b-factor. This is discussed in the next section.

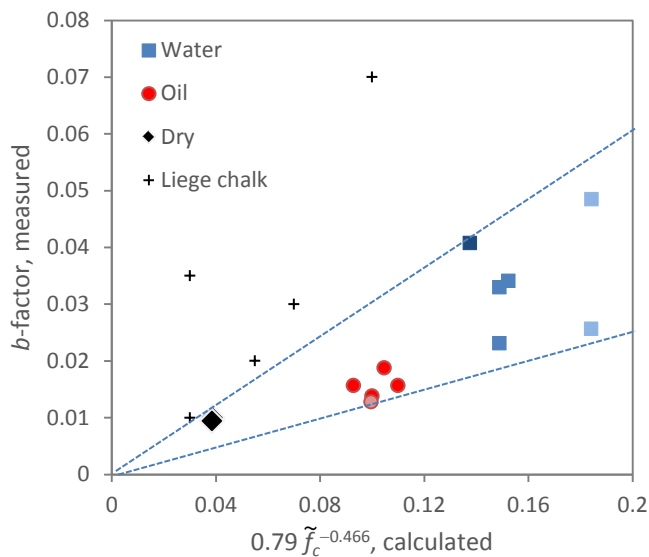


Fig. 4. Measured b-factors vs. the calculated b-factor from Eq. 13. Crosses are Liege chalk results, recalculated from [30], enclosed for comparison. Light colors stand for higher porosity and dark colors for lower porosity than 0.44.

5. DISCUSSION

Several aspects deserve discussion with regards to the application of the Biot critical frequency as a means of enclosing the fluid effect in the b-factor from knowing the fluid density and viscosity.

While the de Waal b-factor is based on uniaxial compaction here it is extracted from unconfined compression tests. Additionally, the rate dependence incorporating the Biot critical frequency is based on oedometer tests. Therefore, the influence by load path on the resulting b-factors should be verified.

There is a higher degree of scattering for the b-factor from the water-saturated specimens and this could be attributed to differences in the specific surface area and permeability indicating small differences in the material. As the permeability is included in the Biot critical frequency this opens for further investigation.

6. CONCLUSION

The experimental results show a correlation exists between data from dry, oil- or water-saturated chalk and an empirical relation with the Biot critical frequency. The critical frequency is interpreted as a measure of the solid-fluid friction.

The Biot critical frequency includes two physical properties of the fluid, which are the viscosity and density. It also includes two material properties, which are the porosity and permeability. All four parameters are normally easily available and measured, leading to an advantage from applying the Biot critical frequency in the determination of the time dependence for high-porosity materials such as reservoir chalk and obtaining the response for either water- or oil-saturated states.

REFERENCES

1. Ruddy, I., M.A. Andersen, P.D. Pattillo, M. Bishlawi, and N. Foged. 1989. Rock Compressibility, Compaction, and Subsidence in a High-Porosity Chalk Reservoir: A Case-Study of Valhall Field. *Journal of Petroleum Technology* 41 (7): 741–746.
2. Rhett, D.W. 1998. Ekofisk Revisited: A New Model of Ekofisk Reservoir Geomechanical Behavior. In *Proceedings of the SPE/ISRM Eurock '98 held in Trondheim, Norway, 8 – 10 July 1998*. Society of Petroleum Engineers: 367–375.
3. de Waal, J.A. and R.M.M. Smits. 1988. Prediction of reservoir compaction and surface subsidence: field application of a new model. *SPE Formation Evaluation, Society of Petroleum Engineers* 3: 347–356.
4. Johnson, J.P. and D.W. Rhett. 1986. Compaction behaviour of Ekofisk chalk as a function of stress. *Society of Petroleum Engineers SPE* 15872: 221–225.
5. Addis, M.A. and M.E. Jones. 1989. Mechanical behaviour and strain rate dependence of high porosity chalk. In *Proceedings of the International Chalk Symposium held at Brighton Polytechnic on 4 – 7 September 1989*, 239–244. London: Thomas Telford.
6. Andersen, M.A., N. Foged and H.F. Pedersen. 1992. The rate-type compaction of a weak North Sea chalk. In *Rock Mechanics Proceedings of the 33rd U.S. Symposium, Santa Fe, New Mexico, 8 – 10 June 1992*, 253–261.
7. Bhandari, A.R. and J. Inoue. 2005. Experimental study of strain rates effects on strain localization characteristics of soft rocks Soils and Foundations. *Journal of the Japanese Geotechnical Society* 45: 125–140.
8. De Gennaro, V., P. Delage, Y.J. Cui, Chr. Schroeder and F. Collin. 2003. Time-dependent behaviour of oil reservoir chalk: A multiphase approach. *Soils and*

- Foundations. Journal of the Japanese Geotechnical Society* 43: 131–147.
9. Dahou, A., J.F. Shao and M. Bederiat. 1995. Experimental and numerical investigations on transient creep of porous chalk. *Mechanics of Materials* 21: 147–158.
 10. Maranini, E. and M. Brignoli. 1999. Creep behaviour of a weak rock: experimental characterization. *International Journal of Rock Mechanics and Mining Sciences* 36: 127–138.
 11. Zhang, X. and C.J. Spiers. 2005. Compaction of granular calcite by pressure solution at room temperature and effects of pore fluid chemistry. *International Journal of Rock Mechanics and Mining Sciences* 42: 950–960.
 12. Andrade, E.N.d.C. 1910. The Viscous Flow in Metals and Allied Phenomena. *Proc. R. Soc. A* 84: 1–12.
 13. Fjær, E., R.M. Holt, P. Horsrud, A.M. Raaen and R. Risnes. 2008. *Petroleum related rock mechanics*. 2nd ed. London: Elsevier.
 14. Jaeger, J.C., N.G.W. Cook and R.W. Zimmerman. *Fundamentals of rock mechanics*. 4th ed. Blackwell Publishing.
 15. Borezi, A.P. and R.J. Schmidt. 2003. *Advanced mechanics of materials*. 6th ed. John Wiley & Sons.
 16. Pharr, G.M. and M.F. Ashby. 1983. On creep enhanced by a liquid phase. *Acta Metallurgica* 31: 129–138.
 17. Sulak, R.M. and J. Danielsen. 1989. Reservoir aspects of Ekofisk subsidence. *Journal of Petroleum Technology, Society of Petroleum Engineers* 41: 709–716.
 18. Mesri, G. and P.M. Godlewski. 1977. Time- and Stress-Compressibility Interrelationship. Journal of the Geotechnical Engineering Division, In *Proceedings of the American Society of Civil Engineers* 103, No. GT5: 417–430.
 19. de Waal, J.A. 1986. On the rate type compaction behaviour of sandstone reservoir rock, Ph.D. thesis, Technische Hogeschool Delft, The Netherlands.
 20. Kolymbas, D. 1977. A Rate-Dependent Constitutive Equation for Soils. *Mech. Res. Comm.* 4(6): 367–372.
 21. Gudehus, G. 2011. Physical Soil Mechanics. In *Series: Advances in Geophysical and Environmental Mechanics and Mathematics*, ed. K. Hutter. Berlin: Springer.
 22. Bourbié, T., O. Coussy and B. Zinzner. 1987. *Acoustics of porous media*. Paris: Editions Technip.
 23. Biot, M. A. 1956. Theory of Propagation of Elastic Waves in a Fluid-Saturated Porous Solid. I. Low-Frequency Range. *The Journal of the Acoustical Society of America* 28: 168–178.
 24. Biot, M. A. 1956. Theory of Propagation of Elastic Waves in a Fluid-Saturated Porous Solid. II. Higher Frequency Range. *The Journal of the Acoustical Society of America* 28: 179–191.
 25. Johnson, D. L., J. Koplik and R. Dashen. 1987. Theory of dynamic permeability and tortuosity in fluid-saturated porous media. *Journal of Fluid Mechanics Digital Archive* 176: 379–402.
 26. Fabricius, I. L., G.T. Bächle, and G.P. Eberli. 2010. Elastic moduli of dry and watersaturated carbonates — effect of depositional texture, porosity and permeability. *Geophysics*. 75(3):N65–N78.
 27. Mavko, G., T. Mukerji and J. Dvorkin. 2009. *The Rock Physics Handbook: Tools for Seismic Analysis in Porous Media*. 2nd ed. Cambridge: Cambridge University Press.
 28. Andreassen, K.A. 2011. Temperature Influence on Rock Mechanical Properties, High-Porosity, Low-Cemented Chalk. Ph.D. thesis. Department of Civil Engineering, Technical University of Denmark.
 29. De Gennaro, V., P. Delage, G. Priol, F. Collin and Y.-J. Cui. 2004. On the collapse behaviour of oil reservoir chalk. *Geotechnique* 54: 415–420.
 30. Priol, G., V.D. Gennaro, P. Delage and T. Servant. 2007. Experimental Investigation on the Time Dependent Behaviour of a Multiphase Chalk. In *Experimental Unsaturated Soil Mechanics*, Berlin: Springer, 112, 161–167.